Electrochemical Membrane Separation of H_2S from Reducing Gas Streams

Jeffrey S. Robinson, D. Scott Smith, and Jack Winnick
Dept. of Chemical Engineering, Georgia Institute of Technology, Atlanta, GA 30332

An improved electrochemical membrane was tested with simulated coal gas having concentrations from 25 to 4,500 ppm H_2S. The process produces elemental hydrogen that enriches the process gas stream at the cathode and elemental sulfur vapor that emerges from the anode. Removal efficiencies average up to 90% at any inlet level; current efficiencies are near 100% at the high inlet concentrations, decreasing significantly at lower H_2S levels as the competing reduction of H_2O becomes more favored. Molten carbonate fuel cell (MCFC) materials can be used exclusively at the MCFC operating temperature of 650°C, with the low concentrations of H_2S, including the NiO cathode. At concentrations higher than about 60 ppm the operating temperature must be lowered approximately 50°C to avoid melting of the sulfided nickel cathode.

Introduction

Membrane gas separation systems have been used in applications, such as hydrogen gas purification, for many years. The separation relies on a chemical potential gradient as the driving force. A pressure or concentration gradient usually provides the necessary driving force for mass transfer of component i across the membrane

$$\Delta\mu_i = \mu_i - \mu_i' = RT \ln\left(\frac{a_i}{a_i'}\right) \tag{1}$$

where the prime represents the extractive side. Typically, these processes are not completely species-selective; therefore, they do not produce high-purity products.

In an electrochemical membrane separation, an electrochemical potential gradient provides the driving force across the membrane:

$$\Delta\overline{\mu} = \overline{\mu_i} - \overline{\mu_i'} = RT \ln\left(\frac{a_i}{a_i'}\right) + z_i F \Delta\Phi \tag{2}$$

which is established by applying an external potential Φ. In this case, with a charged species, a pressure or concentration gradient is neither required nor desired. Application of this principle for the removal of H_2S from coal gas streams is the focus of this paper.

Coal gasification streams may be utilized to generate electricity in a variety of ways (Weaver and Winnick, 1987). H_2S inherent to raw gasification streams must first be removed to acceptable levels. A high-temperature electrochemical membrane separation process is illustrated in Figure 1. This process is advantageous to competing removal technologies because it can be run at or near the coal gasification temperature (Weaver and Winnick, 1987; Alexander and Winnick, 1992). The sour process gas (coal gas containing H_2S), cleansed of particulates, is passed over the cathode. Here the best Lewis acid (electron acceptor) will be reduced. In this case H_2S is favored, resulting in the following

$$H_2S + 2e^- \rightarrow H_2 + S^{2-} \tag{3}$$

A membrane containing sulfide ions in a molten state will act to transport the reduced sulfide ion through the membrane to the anode. Here, if the membrane is capable of preventing diffusion of gases from the cathode side, an inert sweep gas can carry away the oxidized sulfide ions downstream to condense as elemental sulfur. The desired anodic reaction is

$$S^{2-} \rightarrow 1/2S_2 + 2e^- \tag{4}$$

Summing the half-cell reactions 3 and 4 results in the follow-

Correspondence concerning this article should be addressed to J. Winnick.

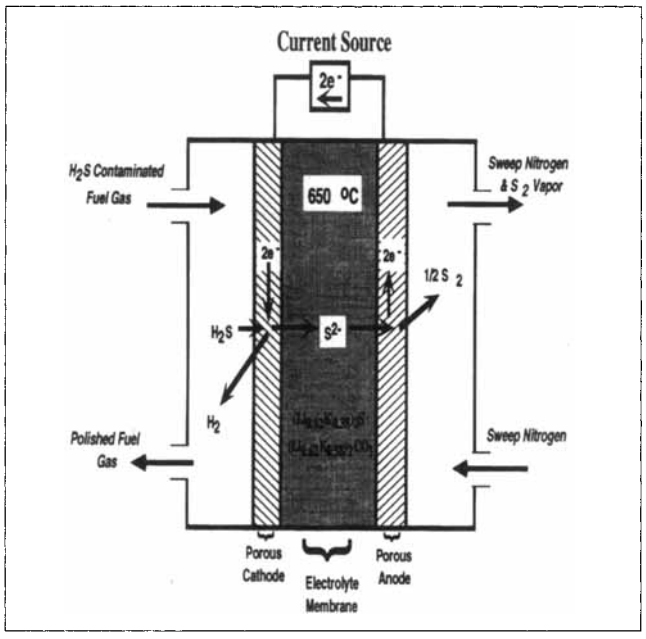

Figure 1. Electrochemical membrane separator (EMS).

ing overall reactions at 923 K

$$H_2S \rightarrow H_2 + 1/2S_2 \tag{5}$$

which can be related to the change in standard Gibb's energy and minimum electrical work required for the separation by

$$W_e = \Delta G = -nFE^\circ \tag{6}$$

where n is the number of electrons transferred in the reaction and F is Faraday's constant or the amount of charge passed per mole of species reduced or oxidized. The relative extent of reaction 5 is determined by chemical equilibrium as expressed by the Nernst relation, a concentration correction to the standard cell potential, E°.

$$E = E_5^\circ - \left(\frac{RT}{nF}\right)\ln\left\{\frac{a_{S^{2-}_{cath}} P_{H_2 cath} P^{1/2}_{S_2 an}}{a_{S^{2-}_{an}} P_{H_2 S_{cath}}}\right\} \tag{7}$$

In addition to the Nernst voltage, additional potential is required to operate the separation cell due to irreversible losses. These losses occur by internal resistance, concentration effects in the process gases, and the activation barrier for electron transfer. The result is the total cell voltage increasing over the reversible potential.

Total cell voltage incorporating ohmic, concentration, and activation polarization along with the Nernst effects (Eq. 7) sums to

$$V_{cell} = \Delta E_{c-a} - |\eta_{conc}| - |\eta_{act}| - \eta_{ohmic} \tag{8}$$

where ΔE_{c-a} is the equilibrium cell voltage.

The situation is somewhat complicated when real gas mixtures are processed. Carbon dioxide and water vapor compete in the reduction reaction at the cathode by

$$CO_2 + H_2O + 2e^- \rightarrow H_2 + CO_3^{2-} \tag{9}$$

The ionic flux through the membrane depends on both the relative mobilities of carbonate and sulfide ions and on their concentrations.

Preventing the oxidation of carbonate at the anode is necessary for prohibiting its transport through the membrane, allowing the preferred oxidation of sulfide ions (reaction 4). This occurs at a standard potential some 700 mV lower than the oxidation of carbonate:

$$CO_3^{2-} \rightarrow CO_2 + 1/2O_2 + 2e^- \tag{10}$$

Summing the commensurable half-cell reactions, shown in Figure 2 on a potential scale, Eqs. 3 and 4 as well as Eqs. 9 and 10 result in the following overall reactions at 923 K:

$$H_2S \rightarrow H_2 + 1/2S_2 \qquad E^\circ = -0.239V \tag{5}$$

and

$$H_2O \rightarrow H_2 + 1/2O_2 \qquad E^\circ = -1.030V \tag{11}$$

The least negative E° requires the smallest amount of voltage input to proceed. Therefore, at low cell potentials only sulfide ions should be transported. Each will occur at the same cell potential, but as expressed by the Nernst relation, the concentration terms will be greatly affected by the large difference in the standard cell potential (E°) values.

$$E = E^\circ_5 - \left(\frac{RT}{nF}\right)\ln\left\{\frac{a_{S^{2-}_{cath}} P_{H_2 cath} P^{1/2}_{S_2 an}}{a_{S^{2-}_{an}} P_{H_2 S_{cath}}}\right\} \tag{7}$$

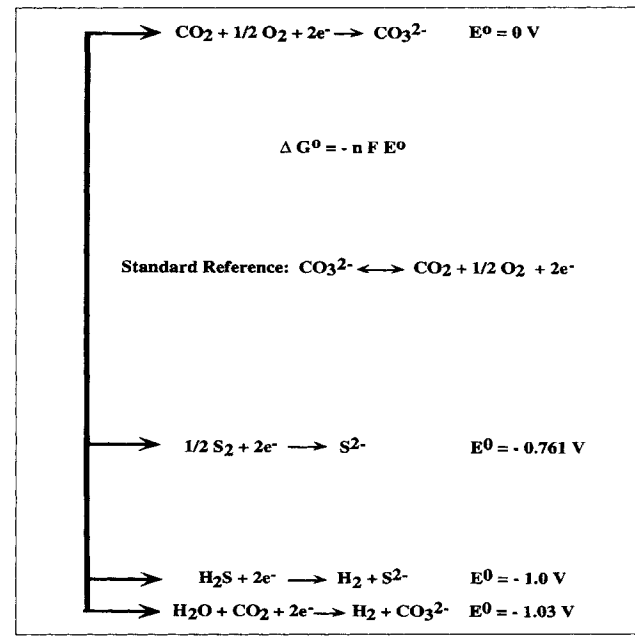

Figure 2. Half-cell reactions on a potential scale (vs. standard reference).

$$E = E^{\circ}_{11} - \left(\frac{RT}{nF}\right)\ln\left\{\frac{a_{CO_{3cath}^{2-}} P_{H_2 cath} P_{CO_2 an} P_{O_2 an}^{1/2}}{a_{CO_{3an}^{2-}} P_{CO_2 cath} P_{H_2O_{cath}}}\right\} \quad (12)$$

For example, assume a process gas is supplied to the cathode with an H_2S level of 100 ppmv, a CO_2 level of 14.2%, and an H_2O level of 5.7%, and that 90% of the H_2S is to be removed via reaction 3. There exists an activity ratio of $a_{CO_3^{2-}}/a_{S^{2-}}$ on the order of 10^5 in the anolyte, assuming equivalent electrode kinetics (Banks and Winnick, 1986; White and Winnick, 1985) for the two reactions, before a significant amount (for example, 1%) of the carbonate is oxidized. When compared to the activity ratio of $a_{CO_3^{2-}}/a_{S^{2-}}$ in the catholyte of 3,000, this shows the thermodynamic preference for the oxidation of S^{2-} to elemental sulfur by Eq. 4.

The transport of H_2S from gas phase to the cathode is limited by film diffusion. The maximum current density i_L permitted is dependent on H_2S concentration

$$i_L = nFk_m \rho \frac{(y_{inlet} - y_{exit})}{\ln\left(\frac{y_{inlet}}{y_{exit}}\right)} \quad (13)$$

while the transport of sulfide ions through the electrolyte-filled membrane is dependent on liquid-phase diffusion

$$i_L = \frac{nFD_{S^{2-}}(C_{S^{2-}}^{cath})}{\delta} \quad (14)$$

Migration of sulfide ions in the imposed field is negligible because of the preponderance of the supporting electrolyte, alkali carbonate. Calculations show that, under the conditions tested, the limiting currents are nearly the same (Robinson, 1996).

Since the carbonate transport of reaction 11 parallels the sulfide transport of reaction 5, the same current is available for transport of both species. Therefore, only a certain amount of current will act to transport either constituent, giving a finite maximum current efficiency with respect to H_2S removal for any percentage of H_2S removed. This is dependent on gas composition and total cross-cell potential required for the desired separation of H_2S. Once the total cross-cell potential is calculated for the desired H_2S removal, the Nernst expression for transport of carbonate (Eq. 12) can be equated to this value, since the relative extent of each occurs at the same potential. The theoretical maximum H_2S current efficiency has been shown (Robinson and Winnick, 1998) to drop to only 99.5% at 90% H_2S removal from 1,000 ppm to 100 ppm H_2S, 93.2% at 90% H_2S removal from 100 ppm to 10 ppm H_2S, and 40.2% at 90% H_2S removal from 10 ppm to 1 ppm H_2S. The excess current goes to reduce water at the cathode and oxidize carbonate at the anode (reactions 9 and 10). However, the thermodynamic preference for sulfide transport over carbonate can be lost if elemental hydrogen passes through the membrane, by molecular diffusion or through macroscopic cracks, from cathode to anode. In this case, the depolarizing effect of the hydrogen at the anode brings about the oxidation of carbonate through the reverse of reaction 9 at about 1 V lower than through reaction 10. This means the standard potential for carbonate oxidation will be nearly the same as for sulfide oxidation, the reverse of reaction 3, as shown in Figure 2. Because the CO_2 and water are in such excess over H_2S, carbonate transport will prevail to the extent of hydrogen crossover, severely lowering the H_2S current efficiency.

Another factor affecting this current efficiency is the availability of H_2S at the cathode–gas interface: that is, the quality of gas-phase mass transfer at this electrode. Mass transfer has been found to be controlled by film diffusion from the bulk gas under normal conditions; that is, with a well-functioning gas-diffusion electrode. If, however, the morphology of this electrode is altered, gas diffusion through this structure may become severely hindered. H_2S levels above 60 ppm in contact with a nickel electrode cause the formation of $Ni_{3\pm x}S_2$, which forms a eutectic with Ni at 640°C (Niu et al., 1994; Weaver and Winnick, 1987), thereby collapsing the pore structure. This effectively diminishes electrode area available for H_2S reduction. Since CO_2 and H_2O are in excess, the current is carried primarily by the parasitic reactions, 9 and 10.

Past work (Lim and Winnick, 1984; Weaver, 1988; Alexander, 1992; and Robinson, 1996) has demonstrated the basic concept and application to a variety of H_2S concentrations. However, current efficiency, especially at high levels of H_2S, has been lower than anticipated. To improve this, the problems described previously, hydrogen crossover and electrode melting, must be addressed. Here we report experiments with improved membranes and lowered temperature of operation, the results of which show dramatically improved efficiency.

Materials and Method

The electrochemical cell apparatus and laboratory setup utilized for bench-scale experiments was similar in design to that of past experiments (Weaver and Winnick, 1987; Alexander and Winnick, 1994); see Figures 3 and 4. Housings of MACOR (machineable ceramic) purchased from Accuratus Corporation (Washington, NJ) were machined into 2×2 in. blocks of 1 in. thickness and utilized at temperatures up to

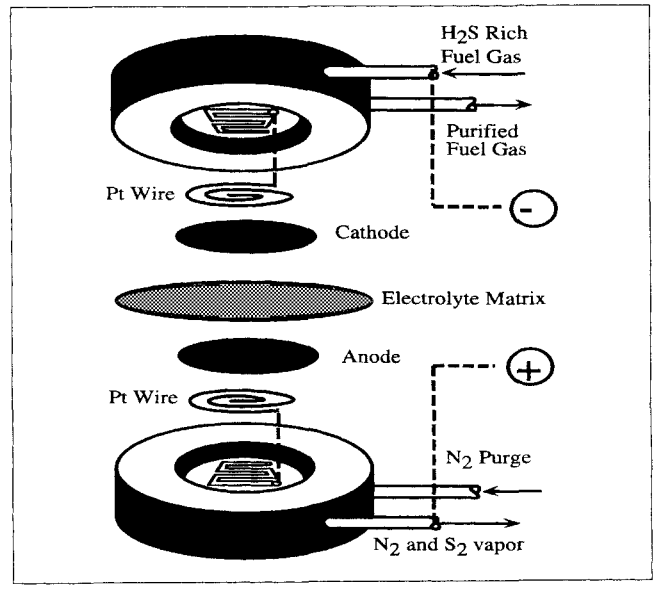

Figure 3. Bench-scale electrochemical cell.

700°C. Housings were machined to encase porous electrodes (surface area = 7.91 cm^2) of 0.9-mm thickness. Gas flowed to the electrode compartments in MACOR housings through 0.32 cm ID alumina tubes purchased from Coors Ceramic Company (Golden, CO). A stainless steel tube was substituted for an alumina tube for the inlet to the cathode cell housing. Flow channels in the electrode compartments were milled 3 mm in width, 3 mm in depth. Electrical connection with electrodes was provided by extending several inches of gold wire (diameter = 0.20 mm) purchased from Englehard (Jackson, MS) through the gas tubing and connecting with a coil of 0.20-mm-diameter platinum wire (Englehard) placed into the electrode well.

Cell housings were separated by a porous ceramic membrane. Ceramic tiles or matrices (membrane and electrolyte) were produced in our laboratory by several methods including particle infiltration, tape-casting, dry pressing, and the Sol-Gel technique (Wanqing et al., 1988). Ceramic tiles were also purchased from outside sources [Gas Research Institute (GRI) (Chicago, IL) and Zircar Corporation (Florida, NY)].

Electrolyte is utilized in the electrochemical system as a pathway of conduction by ions between the electrodes: electrolyte in all bench-scale experiments initially consisted of 62 mol % Li_2CO_3, 38 mol % K_2CO_3 [Fisher Scientific (Norcross, GA)] before the equilibrium reaction (15)

$$(Li_{0.62}K_{0.38})_2CO_3 + H_2S \leftrightarrow (Li_{0.62}K_{0.38})_2S + CO_2 + H_2O \quad (15)$$

The initial amount of electrolyte corresponded to the void volume of the ceramic matrix. The necessary amount was pressed uniaxially (5 MPa) into a thin, 1.25-in.-dia. (32-mm-dia.) disk. This disk was placed on top of the zirconia matrix during cell assembly.

Porous Ni sheets (0.9-mm thickness) were donated to this laboratory by Energy Research Corp (Danbury, CT) (pore size was proprietary but average porosity was ~80%). A 1.25-in. diameter Ni disk was cut from the Ni sheet, soaked in 1-M LiOH, and then dried at 150°C. These were utilized as both the cathode and anode in full-cell operation. The resulting state of the initial Ni electrodes depended on the contacting gas compositions.

The reference electrode consisted of a 0.2-mm-diameter gold wire encased within an alumina tube in contact with the outer portion of the electrolyte tile. Gas containing 3% O_2, 15% CO_2, and balance N_2 was flown by the reference electrode providing the following known, stable half-cell reaction (Vallet and Braunstein, 1979):

$$CO_3^{2-} \rightarrow CO_2 + 1/2O_2 + 2e^- \quad (10)$$

that can be used to compare the anode and cathode reactions.

After the fabrication of electrode and membrane materials, the electrochemical cell was assembled for experimentation. The cell was held together by combustible tape wrapped around the exterior. Once assembled the electrochemical cell was loaded into the furnace; a 1.6-kg stainless steel weight was placed on top for stability and the reference electrode was inserted in contact with the electrolyte tile. Finally, electrical contacts and gas tubes were connected to the current collectors and flow tubes.

On full-cell start-up the initial temperature was set at 150°C. Dry nitrogen was blown through the anode and cathode side of the cell. Temperature was elevated in 10°C intervals, starting from 150°C. Prior to electrolyte melting (490°C), process gas, consisting of specified levels of H_2, CO_2, CO, H_2O, and N_2 was supplied to the cathode side while CO_2 was added to the anode compartment. A temperature increase to 490°C resulted in electrolytic melting coupled with total process-gas seal development (that is, volumetric flow in = volumetric flow out). Melting of the electrolyte was verified by ionic conductivity through the cell, as measured by cross-cell potential stabilization. Process-gas seals were aided by prior application of a thin layer of aluminum to the surface of the housing material around the electrode well. This was accomplished by utilizing aluminum foil or aluminum paint [29 wt. % Al purchased from General Paint & Chemical Company (Cory, IL)] in order to improve the wet gas seal of the cell by intimately binding the membrane structure to the housings with a layer of $LiAlO_2$ formed *in situ*. During the heat-up to run temperature, the aluminum gaskets were converted to Al_2O_3 by

$$2Al + 3/2\,O_2 \rightarrow Al_2O_3 \quad (16)$$

Once the electrolyte became molten (490°C), Al_2O_3 was converted to $LiAlO_2$ through subsequent reaction with Li_2CO_3 in the electrolyte:

$$Al_2O_3 + Li_2CO_3 \rightarrow 2LiAlO_2 + CO_2 \quad (17)$$

Reaction 17 and evaporation are the primary reasons for electrolyte depletion (Robinson, 1996). Additional electrolyte is provided to the matrix via wicking.

The gas stream was hydrated before entering the cell by passing through a steam generator filled with an acidic aqueous solution. The steam generator was held at 50°C to supply ample water for the water–gas shift reaction to take place ($p^{SAT}(H_2O) \sim 0.10$ atm). The gas mixture next passed through a shift reactor (stainless steel tube, FeO catalyst) before entering the cell housing to allow the mixture to reach equilibrium via the water–gas shift reaction:

$$H_2 + CO_2 \leftrightarrow H_2O + CO \quad (18)$$

Process gas equilibrium is verified by comparing cathode outlet CO_2 compositions to thermodynamic calculations.

Once the cell reached run temperature, ionic resistance across the cell was measured by the current-interrupt method. The potentials at the cathode and anode were measured with respect to the reference electrode by multimeters. Evaluation of theoretical CO_2 removal from the process gas (cathode gas) or CO_2 addition in the anode gas with applied current was the first test conducted on the electrochemical membrane separator (EMS). Percentage of CO_2 removal/addition compared to the theoretical value determines system performance.

Once system performance was established, addition of H_2S into the process gas ensued. Baseline exit cathode and anode gas compositions were measured at this point. After calculat-

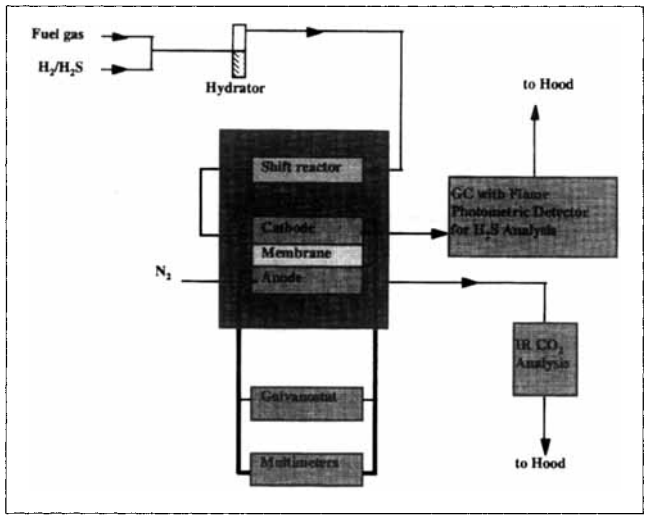

Figure 4. Laboratory setup.

ing limiting current based on mass transfer and active electrode area, current was applied to the cell in a stepwise fashion; the cell was allowed to equilibrate for at least 15 min after each current step. Once equilibrated, potentials with respect to the reference electrode and the exit gas concentrations were measured.

At the completion of the experiment, the electrochemical cell was cooled to room temperature at 100°C/h with only nitrogen flowing into the system. After cool down, the cell was separated and analyzed; this analysis helped identify the intimacy of the electrode and membrane, the condition of these materials, and the electrolyte distribution within the cell. The electrodes were further analyzed by X-ray diffraction to determine their chemical composition. Electron microscopy was also performed to evaluate the morphology of the electrodes and membrane.

Results

H_2S removal experiments were performed on gas compositions representing scrubbed coal gas (25 ppm) as well as sour coal gas compositions (2,500 ppm and 4,500 ppm) for various flow rates. H_2S removal was calculated by:

$$\%\,\text{Removal} = \left[\frac{(H_2S)_{i=0} - (H_2S)_i}{(H_2S)_{i=0}}\right]_{\text{outlet}} \times 100 \qquad (19)$$

These values were calculated on a zero current basis to offset any chemical scrubbing that may occur by the molten carbonate. Current efficiency can then be calculated, as shown by:

$$\eta = \frac{\%\,\text{Removal}_{\text{actual}}}{\%\,\text{Removal}_{\text{theoretical}}} \qquad (20)$$

Removal experiments for scrubbed coal gas and sour coal gas are reported below.

Polishing of contaminant level H_2S from scrubbed coal gas

Run A utilized a Zircar membrane (yttria-stabilized ZrO_2) that had uniform porosity and no warping. The electrolyte was wicked into the membrane at a temperature of 500°C. Once the temperature reached 550°C, in an amount corresponding to a 66% membrane void volume, membrane thickness was measured as 0.5 mm. Aluminum foil gaskets were used on both housings (MACOR) to aid the sealing process. Electrodes were lithiated Ni. After efficient carbonate transport occurred, H_2S was applied to the cell and held at a concentration of 25 ppm. Inlet gases equilibrated to 5.8% CO_2, 25.6% CO, 6.7% H_2O, and 65.3% H_2 after the water–gas shift reaction. The equilibrium sulfide concentration was determined to be 0.11 mol %. Limiting current densities at these conditions were estimated at 2.9 A/m^2 for the gas phase and 17.3 A/m^2 for the membrane. Flow rates varied from 170 cm^3/min to 814 cm^3/min at constant temperature (650°C). At this low H_2S level the NiO electrode will not sulfide; therefore, no melting of the electrode will occur. The higher temperature is advantageous at these low H_2S levels because the equilibrium sulfide content in the electrolyte rises sharply with temperature; as high a sulfide level as possible is desired to eliminate liquid phase sulfide transport limitations.

H_2S removals over 80% were recorded with applied current at four different flow rates, reaching 90% removal at 170 cm^3/min and 580 cm^3/min. Figure 5 illustrates H_2S removals and corresponding current efficiencies versus applied current at the various flow rates. Current efficiency is seen to drop off at the higher removals in accord with the theoretical prediction (Robinson and Winnick, 1998). In all cases, the level of H_2S exiting the cathode after current cessation returned approximately to the level prior to current application.

H_2S removals from sour coal gas

Run B also used a fabricated zirconia membrane. The electrodes were lithiated Ni. Housing materials were MACOR without aluminum sealant. Unlike the polishing removal experiment (Run A), the EMS temperature for sour coal gas experiments was 580°C.

After establishing system permanence through validating carbonate transport, H_2S was added to the gas mixture. Process gases equilibrated, at a cathode flow of 265 cm^3/min, to

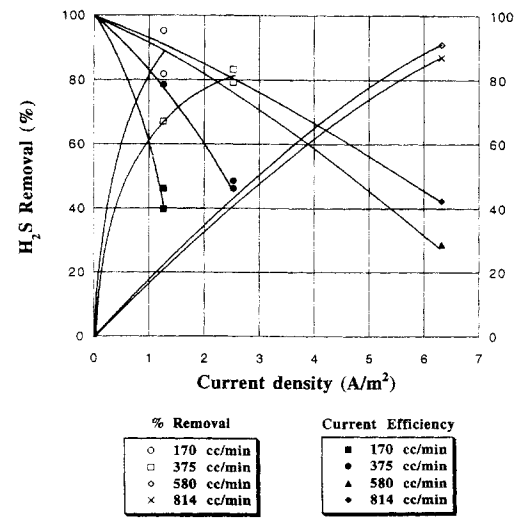

Figure 5. System performance for 25 ppm H_2S inlet.

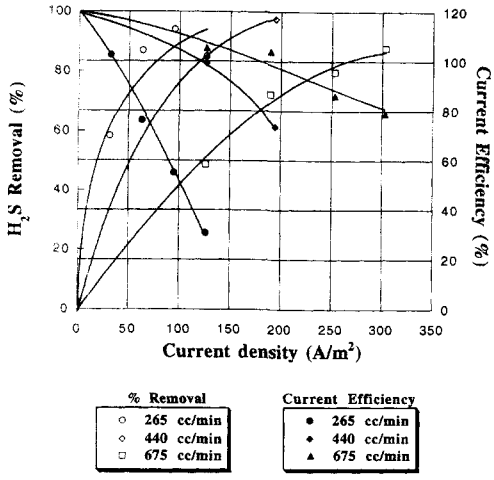

Figure 6. System performance for 2,500 ppm H_2S inlet.

5.6% CO_2, 2.2% CO, 8.3% H_2, 6.7% H_2O, and 2,500 ppm H_2S. Gas-phase limiting current estimated at 342 A/m^2 was one-half the membrane-limiting current density of 684 A/m^2. Electrolyte concentration was calculated to be 93.1 mol % $(Li_{0.68}K_{0.32})_2CO_3$ and 6.9 mol % $(Li_{0.68}K_{0.32})_2S$. Stepwise removal experiments were performed at this flow rate, followed by additional removal experiments at flow rates of 440 cm^3/min and 675 cm^3/min. Internal resistance for all of these flow rates was around 5 ohms. As shown in Figure 6, over 80% removal was achieved at all flow rates attempted. Moreover, current efficiencies remained above 75% at stoichiometric currents necessary for 90% removal for flow rates of 440 and 675 cm^3/min.

In run C, the inlet gas was adjusted to a new concentration of 4,500 ppm H_2S. Gases equilibrated to 12.2% CO_2, 14.5% CO, 21.4% H_2, and 5.6% H_2O, creating an electrolyte concentration of 94.4 mol % $(Li_{0.68}K_{0.32})_2CO_3$, 5.6 mol % $(Li_{0.68}K_{0.32})_2S$. Limiting current densities were 505 A/m^2 in the gas phase and 523 A/m^2 in the membrane. At these concentrations the cathode flow rate was varied from 130 cm^3/min to 570 cm^3/min. Figure 7 demonstrates that around

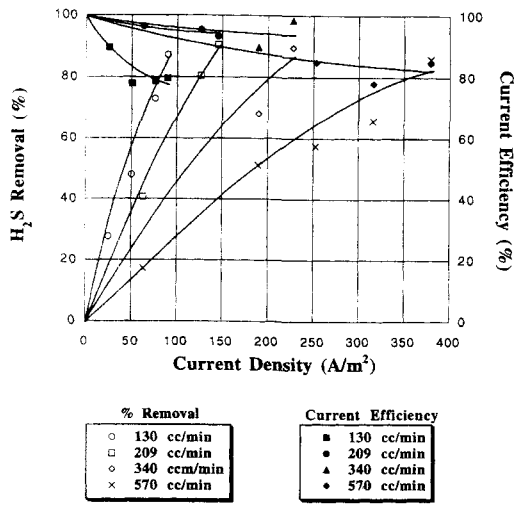

Figure 7. System performance for 4,500 ppm H_2S inlet.

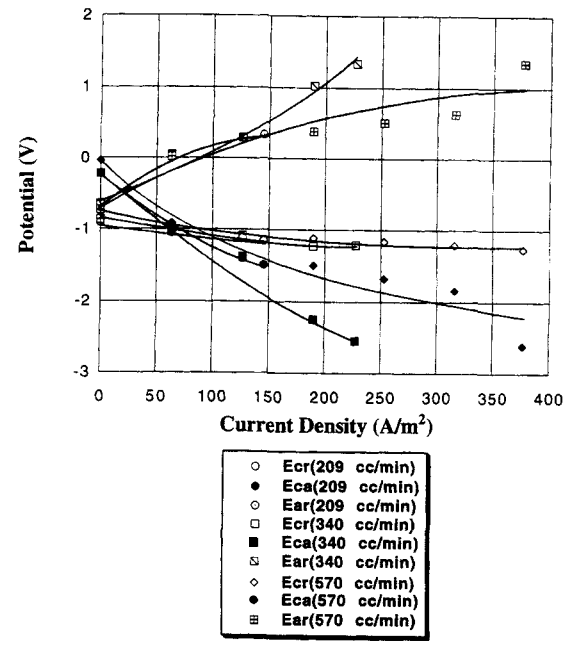

Figure 8. Cell potentials for 4,500 ppm H_2S inlet (not IR compensated).

E_{cr}, E_{ar}, and E_{ca} are potentials of cathode vs. reference, anode vs. reference, and cathode vs. anode, respectively.

90% removal was achieved at four different flow rates, while current efficiencies were above 75% in all cases and above 90% at intermediate flow rates (209 and 340 cm^3/min). Figure 8 illustrates electrode potentials as a function of applied current for different flow rates. E_{cr} (cathode/reference) and E_{ar} (anode/reference) are the electrode potentials vs. the standard carbonate decomposition reference (Eq. 10) while E_{ca} (cathode/anode) is the cross-cell potential. High cross-cell potentials are the direct result of internal resistance, which ranged from 6 to 10 ohms for Run C. Internal resistance should be able to be maintained around 1 ohm with proper cell and electrolyte maintenance. Accounting for ohmic resistances resulted in cross-cell potentials that agreed well with theoretical predictions (Robinson and Winnick, 1998).

Analysis after Runs A–C revealed a three-phase change in the cathode from Ni to a combination of $Ni_{3-x}S_2$, NiS (Millerite), and Ni_3S_2 (Heazlewoodite). 0.03 g of sulfur was recovered from the anode outlet of the cell; verification occurred by heating the powder above its melting point (130°C) creating a viscous garnet liquid.

Discussion

The combination of highly retentive membranes and high-porosity nickel electrodes has permitted removal of H_2S from very low levels in simulated coal gas, despite the high levels of carbon dioxide and water. With a 25 ppm H_2S inlet over 90% removal was obtained at a current efficiency about 40%, near the theoretical maximum (Robinson and Winnick, 1998). The cell voltages at the low current densities required at these low H_2S levels are less than 0.25 V.

At higher H_2S concentrations with operating temperatures decreased to 580°C, the same high removal efficiencies are

found, but at higher current efficiencies. For the 2,500 ppm H_2S feed, the current efficiency is above 80%. The cell voltages here reach nearly 2 V; however, 90% of this is ohmic polarization, which can be minimized in industrial cells. The same behavior is seen at the highest H_2S concentration tested, 4,500 ppm. Once again, high removal efficiency was obtained at high current efficiency. While these current efficiencies are much higher than those seen in earlier studies, they are still below theoretical maxima (Robinson and Winnick, 1998); at these H_2S levels the theoretical current efficiency could reach 99%. The main reason for the improvement is the lowering of the operating temperature to below the melting point of the nickel sulfide. A secondary reason is the improved membrane construction. Slight hydrogen crossover is probably responsible for the small parasitic currents.

The low current efficiency at the very low H_2S levels has little economic impact because of the low current usage at these levels. At the higher H_2S levels, where the main current demand exists, the sharply improved current efficiency gives more credibility to earlier projections of economic viability (Alexander and Winnick, 1994). Further work is necessary to refine the membrane construction so as to minimize parasitic current.

Conclusions

Selective removal of H_2S from simulated coal gasification streams has been demonstrated for both "sour" levels (2,500 ppm H_2S and 4,500 ppm H_2S) and "polished" levels (25 ppm H_2S). Current efficiencies were in accord with theoretical predictions (Robinson and Winnick, 1998) and were somewhat lower at the polished levels than at the sour levels. This highly significant increase in current efficiency obtained for the sour gas removals was primarily due to two revisions from earlier experiments. First, the operating temperature of the process was decreased to 580°C, which is below the melting point of nickel sulfide, thus maintaining electrode morphology and efficient mass transfer. Second, the premanufactured zirconia membrane was more stable and had a consistent pore distribution. This inhibited H_2 crossover from the cathode to the anode, therefore improving the current efficiency.

These new results indicate an even greater economic potential for application to H_2S removal from fuel gas streams, whether natural gas or synthetic gas.

Acknowledgment

The authors would like to thank the United States Department of Energy for their financial support under University Coal Research Grant DE-FG22-94-PC94207.

Literature Cited

Alexander, S., "Electrochemical Removal of H_2S from Fuel Gas Streams," PhD Diss., Georgia Inst. of Technology (1992).

Alexander, S., and J. Winnick, "Electrochemical Polishing of Hydrogen Sulfide from Coal Synthesis Gas," *J. Appl. Electrochem.*, **24**, 1092 (1994).

Banks, E., and J. Winnick, "Electrochemical Reactions of Hydrogen Sulfide in Molten Sulfide," *J. Appl. Electrochem.*, **16**, 583 (1986).

Lim, H. S., and J. Winnick, "Electrochemical Removal and Concentration of Hydrogen Sulfide from Coal Gas," *J. Electrochem. Soc.*, **131**, 562 (1984).

Niu, Y., F. Viani, and F. Gesmundo, "Corrosion of Ni-Nb Alloys in H_2/H_2S Mixtures at 600–800°C," *Corrosion Science*, **36**, 883 (1994).

Reed, J. S., *Introduction to the Principles of Ceramic Processing*, Wiley, New York (1988).

Robinson, J., "Polishing H_2S from Coal Gasification Streams using a High Temperature Electrochemical Membrane Separation Process," PhD Diss., Georgia Inst. of Technology (1996).

Robinson, J., and J. Winnick, "Theoretical Limiting Prediction of H_2S Removal Efficiency from Coal Gasification Streams using an Intermediate Temperature Electrochemical Separation Process," *J. Appl. Electrochem.*, in press (1998).

Vallet, C. E., and J. Braunstein, "Steady-State Composition Profiles in Mixed Molten Salt Electrochemical Devices: II. Molten Carbonate Fuel Cell Analogs," *J. Electrochem. Soc.*, **126**, 527 (1979).

Wanqing, C., R. Gerhardt, and J. B. Watchman, Jr., "Preparation and Sintering of Colloidal Silica-Potassium Silicate Gels," *J. Amer. Ceramic Soc.*, **71**, 1108 (1988).

Weaver, D., "Electrochemical Removal of H_2S from Multi-Component Gas Streams," PhD Diss., Georgia Inst. of Technology (1988).

Weaver, D., and J. Winnick, "Electrochemical Removal of H_2S from Hot Gas Streams," *J. Electrochem. Soc.*, **134**, 2451 (1987).

White, K. A., and J. Winnick, "Electrochemical Removal of Hydrogen Sulfide from Hot Coal Gas: Electrode Kinetics," *Electrochem. Acta.*, **30**, 511 (1985).

Manuscript received Mar. 10, 1998, and revision received July 27, 1998.